

# Inflammatory cell populations in early neuroinflammation in the core and peri-ischemic lesions of rat brain after transient focal cerebral ischemia: A morphometric study

Emoke Horvath<sup>Corresp., 1</sup>, Alex Oradan<sup>2</sup>, Liviu Chiriac<sup>3</sup>, Minodora Dobreanu<sup>4</sup>, Előd-Ernő Nagy<sup>5</sup>, Adina Hutanu<sup>6</sup>

<sup>1</sup> Dept. of Pathology, University of Medicine and Pharmacy of Targu Mures, Targu-Mures, Romania

<sup>2</sup> Laboratory Animal Facility-Center for Experimental Medicine, University of Medicine and Pharmacy of Cluj-Napoca, Cluj-Napoca, Romania

<sup>3</sup> Faculty of Physics, National Magnetic Resonance Center, Babes-Bolyai University of Cluj-Napoca, Cluj-Napoca, Romania

<sup>4</sup> Center for Advanced Medical and Pharmaceutical Research, Department of Laboratory Medicine, University of Medicine and Pharmacy of Targu Mures, Targu-Mures, Romania

<sup>5</sup> Department of Biochemistry, University of Medicine and Pharmacy of Targu Mures, Targu- Mures, Romania

<sup>6</sup> Center for Advanced Medical and Pharmaceutical Research, Department of Laboratory Medicine, University of Medicine and Pharmacy of Targu Mures, Targu- Mures, Romania

Corresponding Author: Eموke Horvath

Email address: emoke.horvath@umftgm.ro

**Background and Objective:** Clinical and experimental observations emphasize the role of inflammation as a direct risk factor for stroke. To better characterize the inflammation, we have conducted a detailed histological analysis of the inflammatory cell population after transient middle cerebral artery occlusion in a rat model.

**Methods:** Fifteen adult Wistar male rats were divided randomly into test (n=10) and sham (n=5) groups. In the ischemic group, transient focal cerebral ischemia was induced with an intraluminal filament technique. Histologic lesions of the ischemic core and the surrounding penumbra zone were evaluated, based on a complex algorithm. Representative morphological changes in the core and the penumbra zone were compared. Immunohistochemistry was performed for leukocytes markers (CD15, CD68, CD3), leukocyte-released effectors (MMP-9 and COX-2), and FXIII (possibly involved in microglia and macrophage activation)

**Results:** Neuronal vacuolation and degeneration were significantly more in the core lesion, whereas cellular edema and inflammatory infiltrate were increased in the penumbra. CD68, CD3, FXIII and Cox-2 expression were significantly higher in the penumbra than in the core (p=0.026; p=0.006; p=0.002; and p<0.001).

**Discussion:** In the rat model of middle cerebral artery occlusion, inflammatory mechanisms, microglia/macrophage cells, and T-lymphocytes likely play an important role in the penumbra. The deterioration of neurons is less in the penumbra than in the core. Appreciation of the role of the inflammatory cells and mechanisms involved in stroke might lead to measures to inhibit the injury and save brain volume.

**Inflammatory cell populations in early neuroinflammation in the core and peri-ischemic lesions of rat brain after transient focal cerebral ischemia: a morphometric study**

**Emőke Horváth<sup>1\*</sup>, Alex Orădan<sup>2</sup>, Liviu Chiriac<sup>3</sup>, Minodora Dobreanu<sup>4,5</sup>, Előd-Ernő Nagy<sup>6</sup> and Adina Hutanu<sup>4,5</sup>**

<sup>1</sup> Department of Pathology, University of Medicine and Pharmacy of Târgu-Mures, Gh. Marinescu Street 38, Târgu-Mures, Romania

<sup>2</sup> Laboratory Animal Facility-Center for Experimental Medicine, Iuliu Hatieganu University of Medicine and Pharmacy, Louis Pasteur Street 6, Cluj-Napoca, Romania

<sup>3</sup> National Magnetic Resonance Center, Faculty of Physics, "Babes-Bolyai" University, Cluj-Napoca, Mihail Kogalniceanu Street 1, Cluj-Napoca, Romania

<sup>4</sup> Center for Advanced Medical and Pharmaceutical Research, University of Medicine and Pharmacy Târgu-Mures, Gh. Marinescu Street 38, Târgu-Mureș, Romania

<sup>5</sup> Department of Laboratory Medicine, University of Medicine and Pharmacy of Târgu-Mureș, Gh. Marinescu Street 50, Târgu-Mures, Romania

<sup>6</sup> Department of Biochemistry, University of Medicine and Pharmacy of Târgu-Mures, Gh. Marinescu Street 38, Târgu-Mures, Romania

\*Corresponding author: Emőke Horváth, Department of Pathology, University of Medicine and Pharmacy of Târgu-Mures. 540136 Gh. Marinescu 38, Târgu-Mures, Romania, e-mail: [emoke.horvath@umftgm.ro](mailto:emoke.horvath@umftgm.ro), [horvath\\_emoke@yahoo.com](mailto:horvath_emoke@yahoo.com), Phone: +40/726221520, Fax:+40-37265325

# 21 ABSTRACT

22 **Background and Objective:** Clinical and experimental observations emphasize the role of  
23 inflammation as a direct risk factor for stroke. To better characterize the inflammation, we have  
24 conducted a detailed histological analysis of the inflammatory cell population after transient  
25 middle cerebral artery occlusion in a rat model.

26 **Methods:** Fifteen adult Wistar male rats were divided randomly into test (n=10) and sham (n=5)  
27 groups. In the ischemic group, transient focal cerebral ischemia was induced with an  
28 intraluminal filament technique. Histologic lesions of the ischemic core and the surrounding  
29 penumbra zone were evaluated, based on a complex algorithm. Representative morphological  
30 changes in the core and the penumbra zone were compared. Immunohistochemistry was  
31 performed for leukocytes markers (CD15, CD68, CD3), leukocyte-released effectors (MMP-9 and  
32 COX-2), and FXIII (possibly involved in microglia and macrophage activation).

33 **Results:** Neuronal vacuolation and degeneration were significantly more in the core lesion,  
34 whereas cellular edema and inflammatory infiltrate were increased in the penumbra. CD68,  
35 CD3, FXIII and Cox-2 expression were significantly higher in the penumbra than in the core  
36 (p=0.026; p=0.006; p=0.002; and p<0.001).

37 **Discussion:** In the rat model of middle cerebral artery occlusion, inflammatory mechanisms,  
38 microglia/macrophage cells, and T-lymphocytes likely play an important role in the penumbra.  
39 The deterioration of neurons is less in the penumbra than in the core.

40 Appreciation of the role of the inflammatory cells and mechanisms involved in stroke might lead  
41 to measures to inhibit the injury and save brain volume.

42 **Keywords:** middle cerebral artery occlusion; transient focal cerebral ischemia; inflammatory  
43 infiltrate; digital morphometry; Cox-2; FXIII

## 44 INTRODUCTION

45 Stroke is the second leading cause of death globally and can lead to permanent disability (*The*  
46 *World Health Organization updates, 2017*). In humans, acute therapy of stroke focuses on  
47 reducing the volume of ischemia and improving the clinical outcome. The therapeutic options  
48 are limited to early recanalization by intravenous thrombolysis with the clot-busting drug,  
49 tissue plasminogen activator administered up to 4.5 hours after the onset of symptoms,  
50 or/and thrombectomy; both methods have a narrow therapeutic window (*Gronberg et al.*  
51 *2013*). The involved parenchyma in acute ischemic stroke has three components: ischemic  
52 core, penumbra, and the region named benign oligoemia, which is characterized by  
53 reduced blood flow. The penumbra is affected by hypoxemia and is at increased risk of  
54 being merged into the ischemic core. Correct estimation of size of the penumbra and  
55 minimizing its extent is critical in guiding stroke therapy. Thus, a focus of acute stroke  
56 intervention should be reperfusion of the penumbra (*Manning et al. 2014; Fuhrer, Günter &*  
57 *Zinke, 2017*).

58 The severity of neural tissue damage after stroke is dependent on duration and intensity of  
59 the ischemia, but also on circulatory independent mechanisms, especially in the peri-  
60 infarct area. Neuronal damage is triggered by chemokines, cytokines, and matrix  
61 metalloproteinases (MMPs) resulting from exocytosis. Inflammatory cell infiltration and  
62 activation in cerebral parenchyma are additional harmful effects (*Wolinski & Glabinski,*  
63 *2013*). Recent clinical observations emphasize the role of inflammation as a direct risk factor for  
64 stroke, and suggest the benefit of anti-inflammatory therapy in reducing the incidence of stroke  
65 in animal models and humans (*Chiba & Umegaki, 2013*).

66 The brain responds to ischemic injury with a complex inflammatory process, characterized by  
67 the participation of resident microglia and blood-derived macrophages, polymorphonuclear  
68 neutrophils (PMNs), and T-lymphocytes. Microglia/macrophages perform phagocytotic functions  
69 and produce neurotropic factors that are involved in neuroprotection. On the other hand,  
70 microglia have cytotoxic activities through secreted neurotoxic substances, reactive oxygen  
71 species and pro-inflammatory cytokines (*Ito et al., 2001; Desestret et al, 2013*). Thus, the  
72 inflammatory process in stroke cannot be categorized as either exclusively beneficial or  
73 detrimental. Study of the inflammatory pathways, with their variety of cells and enzymes  
74 involved in the early stages of neuroinflammation in cerebral ischemia, is difficult to carry out in  
75 humans.

76 We have conducted a detailed histological analysis of the inflammatory cell population after  
77 transient middle cerebral artery occlusion (tMCAO) in a rat model. We determined the extent of  
78 the ischemic area with magnetic resonance imaging (MRI) and a complex algorithm of  
79 neurological assessment. We hypothesize that relationships between the inflammatory cell-  
80 positive area and the neuronal damage are different in the core and the penumbra zone, with  
81 possible implications for targeted therapy.

## 82 MATERIALS AND METHODS

### 83 Rat model of acute focal cerebral ischemia: unilateral transient middle cerebral artery 84 occlusion (tMCAO) and reperfusion

85 The procedures used to create this experimental model were conducted according to the  
86 guidelines for care and use of animals in research (Directive 2010/63/EU of the European  
87 Parliament and the Council on the protection of animals). The study was approved by the Ethics  
88 Committee of the University of Medicine and Pharmacy Târgu-Mures (Ethical Committee  
89 approval number 17/17.03.2016).

90 Initially, 15 healthy adult male Wistar rats of 280 to 320 g, purchased from Laboratory Animal  
91 Facility-Center for Experimental Medicine of University of Medicine and Pharmacy Cluj-Napoca,  
92 Romania, were included in our study. Before and during experiments, the animals were group-  
93 housed (5 animals per cage) in a climate-controlled environment (temperature 21-23°C,  
94 humidity 60%, and natural circadian day-night cycle). All the animals had free access to water  
95 and standard rat chow.

96 The animals were assigned to two groups by a simple randomization. The first group (S,  
97 composed of 5 animals) was assigned to control conditions (Sham group); the second (I,  
98 consisting of 10 animals) was the experimental ischemic (test) group. After two weeks of  
99 accommodation, transient focal cerebral ischemia was induced in the test group by an  
100 intraluminal filament technique: obstruction of the left middle cerebral artery (MCA) for 90  
101 minutes, followed by gentle removal of the filaments, according to the surgical technique we  
102 have described (*Oradan et al., 2017*). All efforts were made to avoid animal suffering.  
103 Postoperative pain was minimized with optimal hydration and subcutaneous tramadol. The  
104 sham-operated group (S), used as controls, was subjected to the same anaesthesia and surgical  
105 procedures without tMCAO. The animals were monitored before, during and after the tMCAO  
106 procedure with rectal temperature recording. Body temperature was maintained with a heating  
107 pad (Docol Corp.). Animals that died during the tMCAO procedure (in post-  
108 ischemic/reperfusion period) were excluded from further study.

### 109 Neurological deficit measurement

110 Behavioural tests for neurological assessment were performed at 90 min (the reperfusion time)  
111 and 24 h after reperfusion by a person blinded to the experiments. An expanded five-point scale  
112 (neuroscore) was used for evaluation of neurological deficit: 0, no deficit; 1, failure to extend  
113 right paw; 2, circling to the right; 3, falling to the right; and 4, inability to walk spontaneously  
114 (*Bederson et al, 1986; Woodruff et al., 2011*). Only animals with a value equal to or greater than  
115 2 points were used for further investigation.

### 116 Brain ischemia control and measurement of infarct volume with MRI

At 24 h after tMCAO, neural tissue damage in each animal (S and I groups) was assessed with MRI (Bruker Bio Spec 70/16 USR scanner, operated at 7 Tesla). After MRI acquisition, the ischemic region was reconstructed and evaluated with 3D Slicer (<https://www.slicer.org/>), an open-source software platform. Animals that had no characteristic signs of ischemia were excluded from the following morphological study. At the end-point of this experiment (24 h after tMCAO), the animals were sacrificed under deep anaesthesia with isoflurane. After vital functions and limb and corneal reflexes were absent (adequate anaesthesia confirmed by the veterinarian), the animals were perfused with 20 ml of 10% formalin through the left ventricle; the brains were removed and kept 24 h in 10% neutral buffered formalin for assessment of the morphological and molecular changes.

### **Morpho-histological analysis and immunohistochemistry**

Twelve animals (5 sham and 7 of the ischemic group) were used for the morphological analysis. Three were excluded; two from the ischemic group (I<sub>1</sub> and I<sub>4</sub>) died after ischemia/reperfusion, and one from the ischemic group (I<sub>3</sub>) had negligible ischemic lesion on MRI examination.

### **Tissue processing and quantification of neural damage**

The brains were processed in rostrocaudal direction, embedded in paraffin wax and cut into 4-5 µm thick sections at multiple levels. The serial sections were stained using haematoxylin and eosin (H&E) complemented with cresyl violet/Nissl (CV) staining to verify the diagnose and anatomic orientation of the ischemic lesion, and to select representative areas for analysis of the histological output in the ischemic core (characterized by the presence of dead neurons) in comparison with penumbra (containing degenerated, yet viable neurons) (Paxinos & Watson, 1986). Adjacent sections to those processed by H&E were selected for immunohistochemistry. The contralateral hemisphere served as negative control.

The cellular modifications induced by acute ischemia changes were examined in sections stained with H&E and CV, particularly in the middle cerebral area. We focused on these morphological cellular and stromal changes: a) focal acute eosinophilic necrosis associated with neural-cell vacuolation; b) neuronal degeneration (pyknotic nuclei associated with vacuolation of neutrophils); c) areas of oedema; and d) the presence of inflammatory cells. For each variable, scores between 1-10 were assigned, as Randell (Randell et al., 2016) have recommended for quantification of brain-tissue damage. To determine the final score, we examined and quantified these variables in the core and penumbra of each sample, using a magnification of 200 x, the score indicating the degree of neural destruction.

### **Immunohistochemistry**

One of all sections with representative neuronal injury was immunostained to establish the rate of glial cell loss (glial fibrillary acidic protein staining), and the immunological profile of inflammatory cell types involved in the focal cerebral ischemia and reperfusion was determined

(neutrophil granulocytes, macrophages and T-cells). We evaluated the core using the following leukocyte markers: anti-CD15 clone Carb-3 (Dako), anti-CD68 EKP1 ab955, anti-CD3 SP7 ab 21703 (Abcam), anti-MMP-9 ab 15W2 (Novocastra), anti COX-2 ab CX-294 (Dako) and anti-Factor XIII a, clone E980.1 (Novocastra). Dilutions were made according to the manufacturers' recommendation, and incubation of the primary antibody was performed overnight. Secondary antibodies were goat anti-mouse IgG and goat anti-rabbit IgG in combination with 3,3'-diaminobenzidine chromogen (DAB) followed by haematoxylin counterstain. As an endogenous control, we used contralateral non-damaged hemisphere tissue. For negative antibody control, normal serum was substituted for the primary antibody.

The H&E and immunostained slides were digitally scanned with Mirax Scanner and examined with the associated Panoramic Viewer 1.15.4 software (3DHISTECH Ltd., Budapest, Hungary). To determine the total tissue damage score (TTDS) for each case, five representative foci from core and penumbra were chosen, captured with a 20x objective, and saved in JPEG format. The effects of acute ischemia on the cell-modification score, and counts of inflammatory cell types, were determined with Image J 1.46 software (National Institutes of Health, Bethesda, MD USA) (Ferreira & Rasband, 2012). The results were calculated individually for each case based on the arithmetic mean.

In the case of immunohistochemically stained slides, in the first phase, we selected the immunopositive cells by colorimetric segmentation followed by measurement of the positive areas in the five selected foci for each case, preceded by conversion of the image from 24-bit RGB format to 8-bit B&W (second phase), for the completely automated analysis. The result was calculated individually for each case based on the arithmetic mean. All specimens (H&E, CV and immunostained) were analysed and assessed individually by two of the authors; if necessary, discrepancies of their findings were discussed, and a consensus was reached.

## Statistical Analysis

Descriptive and comparative statistics were performed with the GraphPad Prism 7.0 1 software (GraphPad Software, Inc.). Between-group comparisons (morphological and immunohistochemical scores) were performed with the non-parametric Mann-Whitney U test. Correlation analysis was performed according to Spearman. The level of statistical significance was set at  $p < 0.05$ .

## RESULTS

### Measurement of neurological deficit

The neuroscore evaluation confirmed the success of the tMCAO procedure. All ischemic-group rats had a score above 2, except one ( $I_3$ ) that had no neurological deficit (score 0) and no MRI signs of ischemia; this animal was excluded from subsequent morphological evaluation and immunohistochemical analysis. All S-group specimens had a neurological deficit score of 0.



## 189 Brain ischemia control measurement using MRI

190 After MRI acquisition, the volume of ischemia in 8 brains subjected to digital image examination  
191 was determined. The median total brain volume (TBV) of group I was 4066.5 mm<sup>3</sup> (min. 3726.94,  
192 max. 5264.65), associated with median ischemic volume (IV) 406.0 mm<sup>3</sup> (min. 10.73, max.  
193 969.9). The median IV/TBV ratio was 0.12 (min. 0.002, max. 0.3). The specimen with a IV/TBV  
194 ratio <0.01 (min. value) was excluded from further studies (specimen I<sub>3</sub> with IV/TBV =0.002).

## 195 Characterization of tissue damage in the cortex: histology and immunohistochemistry

196 One day after stroke was induced, ischemic tissue was clearly demarcated from normal tissue  
197 (Figure 1A and 1B), involving the anatomical region irrigated by the occluded middle cerebral  
198 artery. The histological changes were characterized by eosinophilic coagulation necrosis in the  
199 ischemic core and decrease in glial-fibrillary acidic protein-positive cells (Figure 1C), along with  
200 cell vacuolisation (Figure 1D) and neuronal degeneration (Figure 1 E), oedema and inflammatory  
201 cell infiltration (Figure 1F). In all cases, the contralateral (control) hemisphere had a normal  
202 distribution of glial cells and no ischemic changes in the neural tissue. No representative  
203 morphological modifications were found in the sham group, so this group was not subjected to  
204 quantification of morphological changes.

205 The scores obtained from the morphological characteristics in ischemic group are presented in  
206 Table 1. The median total tissue damage score (TTDS) in the tMCAO group was 23 in the  
207 penumbra (20-27) and 24 (22-27) in the core, not a statistically significant difference (p=0.69).  
208 Scores of cell vacuolization and neuron degeneration were significantly higher in in the core  
209 (p=0.006 and p=0.003), in opposite, cellular oedema and inflammatory infiltration were more  
210 enhanced in the penumbra (p=0.009 and p<0.0001). The most impressive morphological  
211 modification in penumbra was high-grade oedema, while in the core, cell vacuolization and  
212 degenerating neurons dominated. Analyzing the correlation between the ischemic volume/total  
213 brain volume ratio (IV/TBV) and the total tissue damage score (TTDS) in the penumbra and core,  
214 we found no significance (r=-0.18, p=0.70 and r=0.36, p=0.45, respectively).

## 215 Cellular inflammatory response

216 In the first 24 h after tMCAO, signs of inflammatory-cell activation were present in the ischemic  
217 core and the peri-infarction area. Table 2 summarizes the immunological profile of the  
218 inflammatory cell types in the core and penumbra of the ischemic rats 24 h after reperfusion.  
219 CD15+ neutrophils and MMP-9+ cells were the most frequent inflammatory cells in the ischemic  
220 areas, but there was not significant difference between these populations in the penumbra and  
221 core (p>0.05; Table 2). After 24 h survival, CD68-positive and blood-derived macrophages were  
222 relatively few in ischemic tissue. CD 68 positive microglia/macrophage cells, (some of them  
223 expressing FXIII) and CD3 positive T-lymphocytes appeared in damaged tissue (Figure 2 A-F), and  
224 these cells were significantly more numerous in penumbra than in the core (p=0.026 for CD68,



p=0.006 for CD3, respectively; Table 2). In addition, more round FXIII-positive cells appeared in the penumbra zone (p=0.002; Table 2). COX-2 expressing cells (Figure 2 G-H), were also significantly more numerous in penumbra than in the core (p<0.001; Table 2). The positive surface scores of differently expressed markers: CD68, FXIII, CD3 and COX-2 in the core and penumbra are shown as dot-plot representation in Figure 3 A-D.

## DISCUSSION

In this study on tMCAO in a rat model, we evaluated the ischemic core and the penumbra in parallel by morpho-histological and immunohistochemical examination. The inflammatory cell infiltration was more pronounced in the penumbra, and thus we hypothesised a correlation between the inflammatory cell-positive areas in the core and the neuronal damage in the penumbra, occurring within the first 24 hours after transient ischemia.

The dramatically affected brain tissue after tMCAO is the core, with severe morphological changes characterized by intense neuronal cell oedema and degeneration. Hypoxia caused by vascular occlusion leads to decreased energy production with consequent leukocyte activation, massive formation of reactive oxygen species, accumulation of intracellular calcium, and induction of cell membrane injury with neuronal death (Traystman, 2003; Gronberg et al., 2013). This complex mechanism is not limited to the lesion itself, but affects also the perilesional and even remote areas. The region bordering the core, known as the ischemic penumbra, is the region that can be saved if adequate and timely treatment is administered (Popp et al, 2009; Fluri, Schumann & Kleinschitz, 2015).

Human ischemic stroke, usually resulting from middle cerebral artery occlusion, is a multifactorial disease caused by heterogeneous and complex risk factors and conditions, which makes it difficult to reproduce in an animal model. The proximal middle cerebral artery occlusion model induced by direct mechanical occlusion is the most frequently used procedure in stroke research, with high reproducibility, rare complications and focal brain damage like that occurring in human stroke (Bacigaluppi, Comi & Hermann, 2010). Furthermore, the presence of a significant ischemic penumbra early after occlusion makes this technique suitable for neuroprotection studies (Sicard & Fisher, 2009; Canazza et al., 2014).

To mimic all aspects of transient ischemia/reperfusion, we used a microsurgical procedure recommended by Güzel (Güzel et al., 2014), with minor modifications as described (Oradan et al., 2017), followed by a complex algorithm that includes neurological assessment, evaluation by MRI measurement of ischemic-tissue volume, and a histopathological and immunohistochemical examination. Our success rate of inducing an infarction by a 90-minute middle cerebral artery occlusion was 90 % (only one animal had no ischemic lesions according to the MRI examination), in accordance with another report (Bacigaluppi, Comi & Hermann, 2010). With reference to the animal models, the infarction size reportedly is dependent on rat strains: the Wistar strain and

261 the intraluminal filament procedure, using a silicone-coated filament, gives the lowest variability  
262 (*Strom et al., 2013*).

263 We found that the variability of infarction size, measured by MRI was high, but the mean infarct  
264 volume may be related to the volumes of the three t-MCAO-affected areas, as determined with  
265 stereotaxic atlas data. The histological examination confirmed the presence of ischemia, with  
266 more oedema and inflammatory cell infiltration in the penumbra than in the core. The positive  
267 cells were quantified with digital morphometry, a method that greatly improves the  
268 comparability of results.

269 Examining the immunophenotype of inflammatory cells, we found that CD15-positive leucocytes  
270 and MMP9-positive cells constituted most of the cellular elements that infiltrated the damaged  
271 brain tissue after 24-h survival, but without significant difference in cells in the penumbra and  
272 core. The number of positive MMP-9 cells was slightly higher than that of CD15-positive  
273 leucocytes both in the penumbra and core. The grade of neutrophil influx (the main source of  
274 free oxygen radicals), which directly destroys neurons, gains significance through the generation  
275 of post-ischemic tissue damage. The neutrophil granulocytes also produce MMP-9, thus  
276 amplifying the brain-inflammatory response and increasing the extent of the infarction area.  
277 MMP-9 probably mediates degradation of the extracellular matrix, which is followed by  
278 disruption of the blood-brain barrier, with initiation of neuronal death and erythrocyte  
279 extravasation. Regardless of the cellular origin (PMNs, microglia or macrophages), the MMP-9  
280 positive inflammatory cells were the most common cellular elements in the ischemic area. In the  
281 core, both the neutrophils and activated microglia displayed a cellular localization of MMP-9  
282 after ischemic stroke, the microglia presenting a shape and phenotype shift to resemble  
283 macrophage properties. Numerous pro-inflammatory agents triggered by ischemia increase the  
284 MMP expression immediately after a stroke. An increased number of MMP-9 positive cells has  
285 been described not only in the experimental models of cerebral ischemia but also in post  
286 mortem ischemic brain tissue, in association with neutrophil infiltration and activated microglia  
287 cells (*Rosell et al., 2006*). These findings suggest a deleterious role of neutrophils and microglia  
288 in human brain injury (oedema following cerebral acute ischemia) and a potential therapeutic  
289 target in stroke (*Yang & Rosenberg, 2015; Zhang et al., 2017*). In contrast to the significance of  
290 leukocytes, the significance of lymphocytes recruited into the brain after ischemic stroke  
291 remains uncertain. However, recent studies emphasize the role of T-lymphocytes in mediating  
292 reperfusion injury in post-ischemic brain tissue, even though the manner in which lymphocytes  
293 and neutrophils interact in the pathophysiology of stroke is unknown (*Jin, Yang & Li, 2010, Lee et*  
294 *al., 2015*). In our experimental model, after one-day survival, the total T-cell influx in comparison  
295 with neutrophils was reduced. We found a significantly greater CD3-positive cell count in the  
296 penumbra than in the core. Studies on the role of T-cell subsets after stroke (*Jin, Yang & Li,*  
297 *2010*) found an early peak (day 1) in helper T-cells expressing pro-inflammatory cytokines, and a  
298 later peak (day 3 to 7) with cytotoxic T-cells releasing anti-inflammatory cytokines. Stroke  
299 stimulates bone marrow production of myeloid cells, which are recruited to the brain (*Ritzel et*

*al.*, 2015). We detected reduced numbers of CD68-positive macrophages in early infiltrates of both investigated zones, with a stronger expression in the penumbra. Due to phagocytotic activity, these cells remove cellular debris and, like neutrophils, recruit and activate lymphocytes (Gronberg *et al.*, 2013). Resident microglia cells are activated rapidly on day 1 after focal cerebral ischemia. In contrast, blood-derived macrophages are rare on day 2, as they infiltrate the damaged brain tissue 24-48 hours after focal cerebral. In their activated status in the penumbra, these cells shift from a thin, ramified morphology to a large, amoeboid structure, reflecting their activation (Lee *et al.*, 2014; Ritzel *et al.*, 2015).

We found that part of the CD68-positive cells with macrophage and amoeboid microglia morphology express coagulation factor XIII (FXIII), with a significant difference in number of these cells between the positive surfaces in the penumbra and the core. Based on this result, we hypothesised that FXIII is involved in the activation of these cells. Recently, FXIII-A was reported to be a good marker of macrophage alternative pathway activation, but the interaction of coagulation factor FXIII with cells of the immune system has been demonstrated infrequently (Navarrete *et al.*, 2014). This relationship includes the modification of FXIII expression during monocyte differentiation and monocyte-macrophage activation, and is supported by the presence of FXIII in the cytoplasm of monocytes/macrophages with phagocytic potential. Cytoplasmic FXIII (cFXIII) is implicated in phagocytosis, and the effect of monocyte activation on cFXIII expression depends on the activation pathway: the classical pathway down-regulates cFXIII expression, while the alternative pathway up-regulates it (Bagoly, Katona & Muszbek, 2012). cFXIII produced by macrophages from the penumbra and core is a substrate for neutrophil elastase released by activated PMNs, inducing a limited cleavage of cFXIII, which results in enzyme activation, followed by a much slower proteolytic inactivation (Bagoly *et al.*, 2008).

Cyclooxygenase-2 (COX-2) is an inflammatory signal-induced key enzyme in arachidonic acid metabolism, being induced in normal cell types, including blood-derived macrophages, microglia, and endothelial cells in response to inflammatory cytokines (Patrono, 2016). COX-2 expression in ischemic tissue is quickly up-regulated after tMCAO together with MMP-2 and MMP-9 activity. Increased levels of COX-2 increase the level of prostaglandin E, with tissue destruction and early development of oedema (Kim *et al.*, 2017). In our study, we found significantly higher COX-2- positive surface area in the penumbra than in the core. The high COX-2-positive area in comparison with the CD68-positive surface is probably due to the appearance of numerous microglia and macrophages in the penumbra and core, activated through a dual pathway (classical and alternative), but also to CD15-positive neutrophils. PGE-2, which is the product of COX-2 activity, is involved in the early development of high-grade oedema, which in our experiments was the most representative morphological modification in the penumbra, with less in the core.

Our study has limitations. First, in the t-MCAO model, primary core damage may recover, and a secondary delayed injury evolves after a free interval of up to 12 hours. This is a long therapeutic

window that is not seen in human stroke, an important difference between human and experimental stroke pathways, as described by Hossmann (Hossmann, 2012). Second, we did not perform a time-dependent characterization of the inflammatory response. Lacking the determination of M1/M2 polarization of macrophages and microglia, we could not collect data referable to the rate of the pro-inflammatory (M1)/anti-inflammatory (M2) character type. Considering that M1 and M2 macrophages and microglia can be converted into each other in their specific microenvironment, polarization of macrophages and microglia plays an important role in controlling the balance between the induction and suppression of inflammation (Nakagawa & Chiba, 2014). Therefore, the role of cFXIII in macrophage activation needs further investigation.

## CONCLUSION

Applying digital morphometry in an experimental rat model of cerebral ischemia, we determined that microglia/macrophage subsets and T-lymphocytes were present in the penumbra zone. We elucidated a higher grade of cellular vacuolization and neuronal degeneration in the core lesion, whereas cellular oedema, macrophage and T-cell infiltration were more intense in the penumbra. Significantly higher Cox-2 and cytoplasmic FXIII expression was present in the penumbra zone. The early inhibition of these cells and regulatory factors with pro-inflammatory properties may decrease the extent of the penumbra zone and enlarge the narrow therapeutic window in the first 24 hours of ischemic stroke.

## 357 FUNDING SOURCES

358 This research was supported by an Internal Research Grant from the University of Medicine and  
359 Pharmacy Târgu-Mures, Romania (Number 17803/1/22.12.2015). The authors thank the  
360 Studium Prospero Foundation (Romania) for partial financial support.

## 361 ACKNOWLEDGEMENTS

362 The morphological and immunohistochemical analyses used the infrastructure of the Advanced  
363 Medical and Pharmaceutical Research Center of the University of Medicine and Pharmacy Târgu-  
364 Mureş.

## 365 COMPETING FINANCIAL INTERESTS

366 The authors declare that they have no conflicts of interests.

## 367 REFERENCES

- 368 Bacigaluppi M, Comi G, Hermann DM. 2010. Animal Models of Ischemic Stroke. Part Two:  
369 Modelling Cerebral Ischemia. *The Open Neurol J.* 4:34-38.  
370 <https://dx.doi.org/10.2174%2F1874205X01004020034>.
- 371 Bagoly Z, Fazakas F, Komaromi I, Haramura G, Toth E, and Muszbek L. 2008. Cleavage of factor  
372 XIII by human neutrophil elastase results in a novel active truncated form of factor XIII A subunit.  
373 *Thrombosis and Haemostasis* 99:668-674. 10.1160/th07-09-0577
- 374 Bagoly Z, Katona E, and Muszbek L. 2012. Factor XIII and inflammatory cells. *Thrombosis*  
375 *Research* 129:S77-S81. 10.1016/j.thromres.2012.02.040
- 376 Bederson JB, Pitts LH, Tsuji M, Nishimura MC, Davis RL, and Bartkowski H. 1986. Rat middle  
377 cerebral-artery occlusion- evaluation of the model and development of a neurologic  
378 examination. *Stroke* 17:472-476. 10.1161/01.str.17.3.472
- 379 Canazza A, Minati L, Boffano C, Parati E, and Binks S. 2014. Experimental models of brain  
380 ischemia: a review of techniques, magnetic resonance imaging, and investigational cell-based  
381 therapies. *Frontiers in Neurology* 5. 10.3389/fneur.2014.00019
- 382 Chiba T, and Umegaki K. 2013. Pivotal Roles of Monocytes/Macrophages in Stroke. *Mediators of*  
383 *Inflammation* 10.1155/2013/759103
- 384 Desestret V, Riou A, Chauveau F, Cho TH, Devillard E, Marinescu M, Ferrera R, Rey C, Chanal M,  
385 Angoulvant D, Honnorat J, Nighoghossian N, Berthezene Y, Nataf S, and Wiart M. 2013. In Vitro  
386 and In Vivo Models of Cerebral Ischemia Show Discrepancy in Therapeutic Effects of M2  
387 Macrophages. *Plos One* 8. 10.1371/journal.pone.0067063

- 388 Ferreira T, Rasband W. 2012. ImageJ User Guide. Image processing and analysis in Java. National  
389 Institutes of Health, <http://rsb.info.nih.gov/ij>.
- 390 Fluri F, Schuhmann MK, and Kleinschnitz C. 2015. Animal models of ischemic stroke and their  
391 application in clinical research. *Drug Design Development and Therapy* 9:3445-3454.  
392 10.2147/dddt.s56071
- 393 Fuhrer H, Gunther A, Zinke J, Niesen WD, and Grp IS. 2017. Optimizing Cardiac Out-Put to  
394 Increase Cerebral Penumbra Perfusion in Large Middle Cerebral Artery Ischemic Lesion-  
395 OPTIMAL Study. *Frontiers in Neurology* 8. 10.3389/fneur.2017.00402
- 396 Gronberg NV, Johansen FF, Kristiansen U, and Hasseldam H. 2013. Leukocyte infiltration in  
397 experimental stroke. *Journal of Neuroinflammation* 10. 10.1186/1742-2094-10-115
- 398 Güzel A, Rölz R, Nikkhah G, Kahlert UD, Maciaczyk J. 2014. A microsurgical procedure for middle  
399 cerebral artery occlusion by intraluminal monofilament insertion technique in the rat: a special  
400 emphasis on the methodology. *Exp. Transl. Stroke Med.* 6 e6,  
401 <https://dx.doi.org/10.1186%2F2040-7378-6-6>.
- 402 Hossmann KA. 2012. The two pathophysiologies of focal brain ischemia: implications for  
403 translational stroke research. *Journal of Cerebral Blood Flow and Metabolism* 32:1310-1316.  
404 10.1038/jcbfm.2011.186
- 405 Ito D, Tanaka K, Suzuki S, Dembo T, and Fukuuchi Y. 2001. Enhanced expression of Iba1, ionized  
406 calcium-binding adapter molecule 1, after transient focal cerebral ischemia in rat brain. *Stroke*  
407 32:1208-1215. 10.1161/01.str.32.5.1208
- 408 Jin R, Yang GJ, and Li GH. 2010. Inflammatory mechanisms in ischemic stroke: role of  
409 inflammatory cells. *Journal of Leukocyte Biology* 87:779-789. 10.1189/jlb.1109766
- 410 Kim S, Jeong J, Jung H-S, Kim B, Kim YE, Lim DS, Kim SD and Song YS. 2017. Anti-inflammatory  
411 effect of Glucagon-like Peptide-1 Receptor Agonist, Exendin-4, through modulation of IB1/J1P1  
412 expression and JNK Signalling in stroke. *Exp Neurobiol* 26(4): 227-239. doi:  
413 10.5607/en.2017.26.4.227.
- 414 Lee Y, Lee SR, Choi SS, Yeo HG, Chang KT, and Lee HJ. 2014. Therapeutically Targeting  
415 Neuroinflammation and Microglia after Acute Ischemic Stroke. *Biomed Research International*  
416 10.1155/2014/297241
- 417 Manning NW, Campbell BCV, Oxley TJ, and Chapot R. 2014. Acute Ischemic Stroke Time,  
418 Penumbra, and Reperfusion. *Stroke* 45:640-644. 10.1161/strokeaha.113.003798



- 419 Nakagawa Y, Chiba K. 2014. Role of microglial M1/M2 polarisation in relapse and remission of  
420 psychiatric disorders and diseases. *Pharmaceuticals (Basel)* 7(12):1028-1048, doi:  
421 10.3390/ph7121028.
- 422 Navarrete M, Garcia J, Dutzan N, Henriquez L, Puente J, Carvajal P, Hernandez M, and Gamonal J.  
423 2014. Interferon-gamma, Interleukins-6 and -4, and Factor XIII-A as Indirect Markers of the  
424 Classical and Alternative Macrophage Activation Pathways in Chronic Periodontitis. *Journal of*  
425 *Periodontology* 85:751-760. 10.1902/jop.2013.130078
- 426 Oradan A, Hutanu A, Horvath E, Chiriac L, and Dobreanu M. 2017. Improved rat stroke model by  
427 intraluminal middle cerebral artery occlusion: a special emphasis on surgical technique. *Health*  
428 *Problems of Civilization* 11:202-210. 10.5114/hpc.2017.70008
- 429 Patrono C. 2016. Cardiovascular effects of cyclooxygenase-2 inhibitors: a mechanistic and clinical  
430 perspective. *British Journal of Clinical Pharmacology* 82:957-964. 10.1111/bcp.13048
- 431 Paxinos G, Watson C. 1986. The Rat Brain in Stereotaxic Coordinates. 2nd ed. San Diego,  
432 California Academic Press.
- 433 Popp A, Jaenisch N, Witte OW, and Frahm C. 2009. Identification of Ischemic Regions in a Rat  
434 Model of Stroke. *Plos One* 4. 10.1371/journal.pone.0004764
- 435 Randell A, Chokshi K, Kane B, Chang H, Naiel S, Dickhout JG, and Daneshtalab N. 2016.  
436 Alterations to the middle cerebral artery of the hypertensive-arthritic rat model potentiates  
437 intracerebral hemorrhage. *Peerj* 4. 10.7717/peerj.2608
- 438 Ritzel RM, Patel AR, Grenier JM, Crapser J, Verma R, Jellison ER, and McCullough LD. 2015.  
439 Functional differences between microglia and monocytes after ischemic stroke. *Journal of*  
440 *Neuroinflammation* 12. 10.1186/s12974-015-0329-1
- 441 Rosell A, Ortega-Aznar A, Alvarez-Sabin J, Fernandez-Cadenas I, Ribo M, Molina CA, Lo EH, and  
442 Montaner J. 2006. Increased brain expression of matrix metalloproteinase-9 after ischemic and  
443 hemorrhagic human stroke. *Stroke* 37:1399-1406. 10.1161/01.STR.0000223001.06264.af
- 444 Sicard KM, Fisher M. 2009. Animal models of focal brain ischemia. *Exp Transl Stroke Med.* 1e7,  
445 <https://dx.doi.org/10.1186%2F2040-7378-1-7>
- 446 Strom JO, Ingberg E, Theodorsson A, and Theodorsson E. 2013. Method parameters' impact on  
447 mortality and variability in rat stroke experiments: a meta-analysis. *Bmc Neuroscience* 14.  
448 10.1186/1471-2202-14-41
- 449 The World Health Organization (WHO) updates fact sheet on Top 10 causes of Death,  
450 [https://communitymedicine4asses.wordpress.com/2017/02/01/who-updates-fact-sheet-on-top-](https://communitymedicine4asses.wordpress.com/2017/02/01/who-updates-fact-sheet-on-top-10-causes-of-death-27-january-2017/)  
451 [10-causes-of-death-27-january-2017/](https://communitymedicine4asses.wordpress.com/2017/02/01/who-updates-fact-sheet-on-top-10-causes-of-death-27-january-2017/)



- 452 Traystman RJ. 2003. Animal models of focal and global cerebral ischemia. *Ilar Journal* 44:85-95.  
453 10.1093/ilar.44.2.85
- 454 Wolinski P, and Glabinski A. 2013. Chemokines and Neurodegeneration in the Early Stage of  
455 Experimental Ischemic Stroke. *Mediators of Inflammation* 10.1155/2013/727189
- 456 Woodruff TM, Thundyil J, Tang SC, Sobey CG, Taylor SM, and Arumugam TV. 2011.  
457 Pathophysiology, treatment, and animal and cellular models of human ischemic stroke.  
458 *Molecular Neurodegeneration* 6. 10.1186/1750-1326-6-11
- 459 Yang Y, and Rosenberg GA. 2015. Matrix metalloproteinases as therapeutic targets for stroke.  
460 *Brain Research* 1623:30-38. 10.1016/j.brainres.2015.04.024
- 461 Zhang HT, Zhang P, Gao Y, Li CL, Wang HJ, Chen LC, Feng Y, Li RY, Li YL, and Jiang CL. 2017. Early  
462 VEGF inhibition attenuates blood-brain barrier disruption in ischemic rat brains by regulating the  
463 expression of MMPs. *Molecular Medicine Reports* 15:57-64. 10.3892/mmr.2016.5974

## Table 1 (on next page)

Results of the comparative study based on the applied score system (cell vacuolation, neural degeneration, cellular edema and inflammatory infiltration) for the core and penumbra.

Co-core. P-penumbra. Score A- cell vacuolization. Score B- neuronal degeneration. Score C- cellular oedema. Score D -inflammatory infiltration. IV-ischemic volume. TBV-total brain volume. \*Mann-Whitney U test.

Ischemic Group (n=7)	Score A		Score B		Score C		Score D		Total Tissue Damage Score		IV/TBV ratio
	P	Co	P	Co	P	Co	P	Co	P	Co	
I <sub>2</sub>	6	9	7	8	9	6	5	3	27	26	0.01
I <sub>5</sub>	4	8	5	6	9	6	5	2	23	22	0.1
I <sub>6</sub>	7	9	4	8	9	8	4	2	24	27	0.25
I <sub>7</sub>	6	9	6	7	8	7	6	3	26	26	0.19
I <sub>8</sub>	4	7	4	8	8	5	4	3	20	23	0.12
I <sub>9</sub>	6	9	5	9	7	4	5	2	23	24	0.3
I <sub>10</sub>	6	6	4	8	7	6	6	3	23	23	0.1
Median (min.-max.)	6 4-7	9 6-9	5 4-7	8 6-9	8 7-9	6 4-8	5 4-6	3 2-3	23 20-27	24 22-27	0.12 (0.01-0.3)
p*	0.006		0.003		0.009		<0.0001		0.69		

## Table 2 (on next page)

The immunological profile of inflammatory cell types represented by median (min-max) value positive cell surface (% of the total area) in the core and penumbra of the ischemic-rat group (n=7).

\*p values calculated by Mann-Whitney U test.

Inflammatory Cell Type	% positive cells/total examined area	
	Penumbra	Core
Neutrophils (CD15+)	6.13 (5.52-7.36)	5.5 (3.92-7.7)
	p=0.274	
Macrophages (CD68+)	2.68 (1.87-2.95)	1.91 (1.78-2.03)
	p=0.026	
FXIII+	1.67 (1.34-2.26)	1.27 (0.92-1.49)
	p=0.002	
T-Cells (CD 3+)	1.48 (1.26-1.56)	1.08 (0.87-1.49)
	p=0.006	
MMP-9+	7.53 (7.32-7.83)	7.81 (7.26-8.12)
	p=0.4	
COX-2+	5.13 (4.96-5.55)	3.7 (3.57-4.18)
	p<0.001	

# Figure 1

Representative morphological features of tMCAO-induced ischemia around the middle cerebral area.

**(A)** Clearly demarcated ischemic zone in the ipsilateral cerebral cortex and thalamus represents the penumbra, surrounding the core (red arrows), Nissl staining, 1x obj. **(B)** Core (c) and penumbra (p) interface viewed with H&E staining, 4x.obj. **(C)** Decrease of the Glial-fibrillary acidic protein-positive astrocytes in the ischemic core, DAB staining, 10x obj. **(D)** The most impressive morphological modifications in the ischemic core: focal acute necrosis associated with neural-cell vacuolation (red arrows), and **(E)** Neural degeneration associated with vacuolation of neuropil (red arrows), Nissl staining, 20x obj. **(F)** Penumbra zone with areas of edema (red arrows) and inflammatory cell infiltration (circle), Nissl staining, 10x obj.

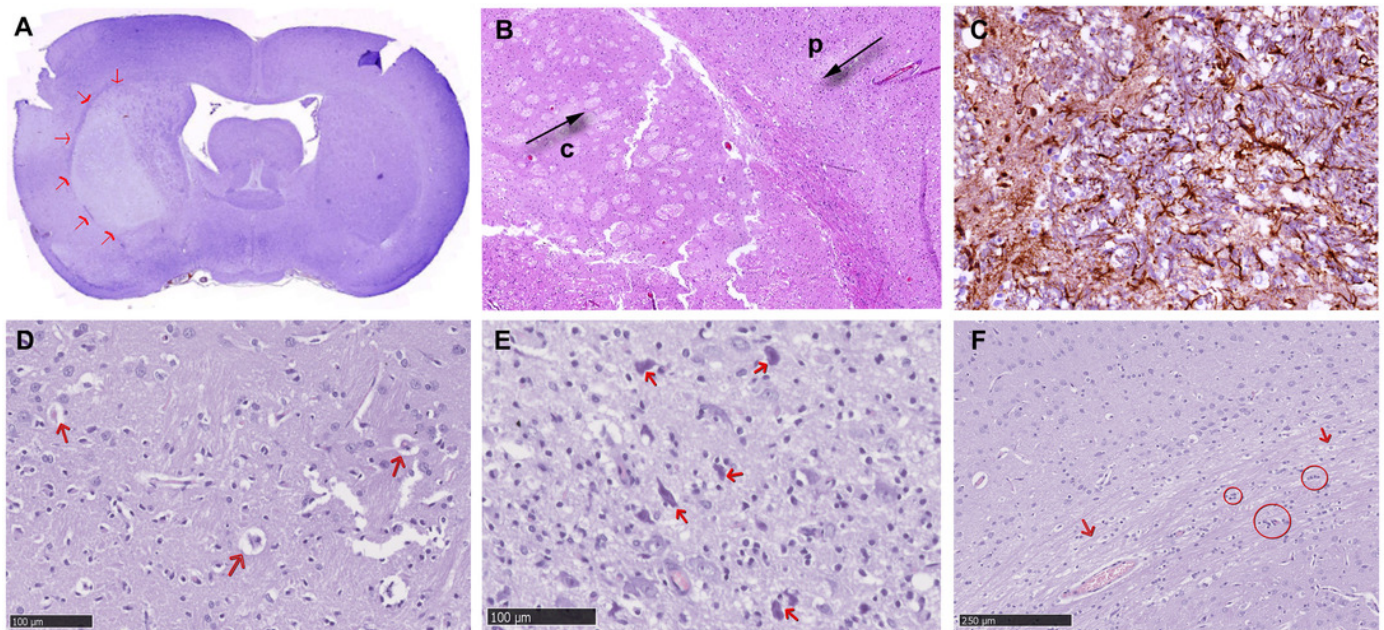




# Figure 2

The immunological profile of the inflammatory cell types, with significantly higher positive surface area (calculated morphometrically by Image J) in the penumbra than in the ischemic core, after 24 h survival following tMCAO (DAB chromogen, 20x).

Fewer CD68-positive macrophages in the core **(A)** than in the penumbra **(B)**. Rare, round FXIII-positive cells in the core **(C)** in comparison with the peri-ischemic area **(D)**, associated with reduced influx of CD3 positive T-cells both in the ischemic core **(E)** and penumbra zone **(F)**. Areas infiltrated by inflammatory elements with COX-2 immunophenotype in core **(G)** and penumbra **(H)**.

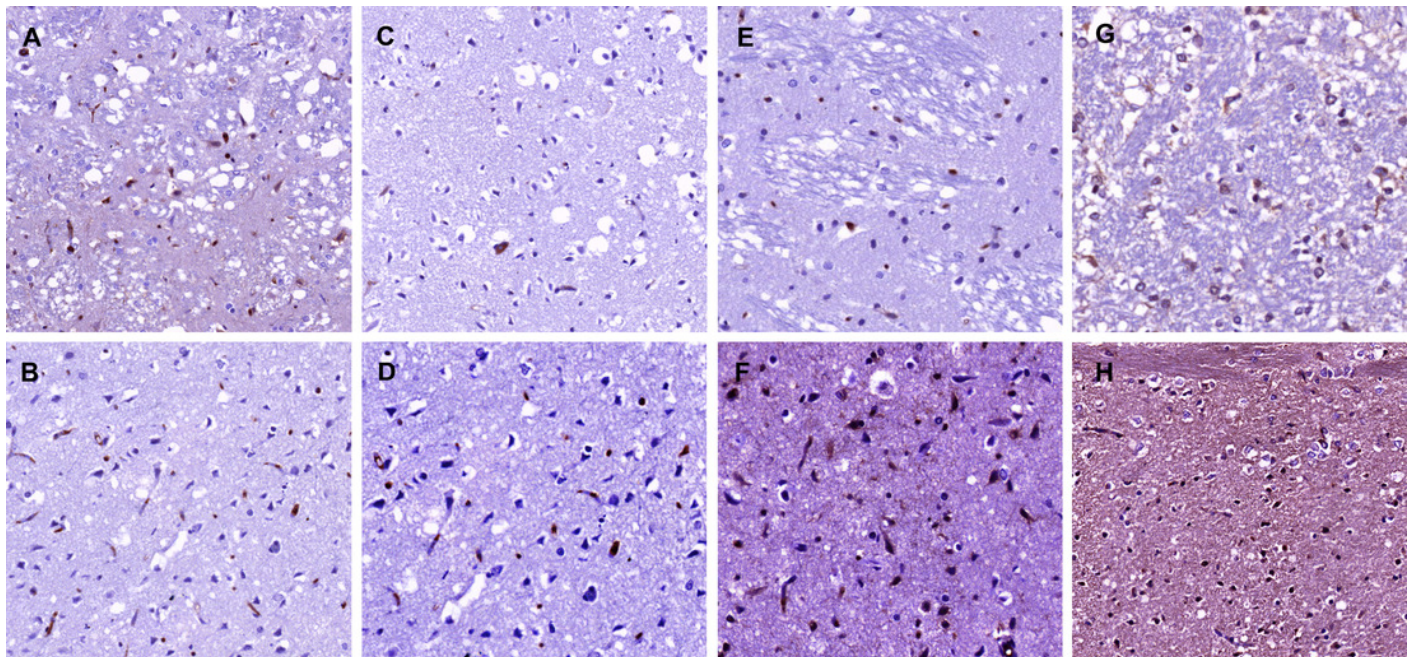




### Figure 3(on next page)

Comparative dot-plot representations of significantly different inflammatory cell markers. (A) CD68, (B) FXIII, (C) CD3 and (D) Cox-2.

p – penumbra, co – core; all markers represented as % of the positive surface area, shown as median and 95% CI, \*  $p < 0.05$ , \*\*  $p < 0.01$ , \*\*\*  $p < 0.001$ , calculated by the Mann-Whitney U test.

